RSC Advances

PAPER

View Article Online
View Journal | View Issue

Cite this: *RSC Adv.*, 2023, **13**, 18443

Balancing "on" and "off" response of hydroxyl groups to a nanozyme-catalyzing system for the construction of an ultra-sensitive and selective "signal-on" detection platform for dopamine†

Hongmei Lan,‡[a] Gaoya Li,‡[a] Guo Chen,[ab] Mengyao Ding,[a] Shuangling Xiao,[a] Jianglin Xiang,[a] Xingwu Duan,[a] Haiyan Cao,[a] Wenbing Shi[a] and Wenfei Dong*[a]

Targeting the functional groups present in analytes by nanozyme-catalyzed systems is a promising strategy to construct sensitive and selective platforms for the sensing of specific analytes. Herein, various groups (–COOH, –CHO, –OH, and $–NH_2$) on benzene were introduced in an Fe-based nanozyme system with MoS_2–MIL-101(Fe) as the model peroxidase nanozyme, H_2O_2 as the oxidizing agent, and TMB as the chromogenic substrate, and the effects of these groups at both a low concentration and high concentration were further investigated. It was found that the hydroxyl group-based substance catechol showed an "on" effect at a low concentration to increase the catalytic rate and enhance the absorbance signal, whereas an "off" effect at a high concentration with a decreased absorbance signal. Based on these results, the "on" mode and "off" mode for the biological molecule dopamine, a type of catechol derivative, were proposed. In the control system, MoS_2–MIL-101(Fe) catalyzed the decomposition of H_2O_2 to produce ROS, which further oxidized TMB. In the "on" mode, the hydroxyl groups of dopamine could combine with the Fe(III) site of the nanozyme to lower its oxidation state, resulting in higher catalytic activity. In the "off" mode, the excess dopamine could consume ROS, which inhibited the catalytic process. Under the optimal conditions, by balancing the "on" and "off" modes, the "on" mode for the detection of dopamine was found to have better sensitivity and selectivity. The LOD was as low as 0.5 nM. This detection platform was successfully applied for the detection of dopamine in human serum with satisfactory recovery. Our results can pave the way for the design of nanozyme sensing systems with sensitivity and selectivity.

Received 4th May 2023
Accepted 30th May 2023

DOI: 10.1039/d3ra02946h

rsc.li/rsc-advances

1 Introduction

Natural enzymes with high catalytic activity and precise substrate specificity have been widely used in the field of analytical sensing.[1–3] However, they also show the intrinsic disadvantages of easy inactivation, difficult purification, and high cost, prompting research on the development of stable and cheap alternatives to natural enzymes. As a new generation of enzyme alternatives, nanozymes, which are defined as nanomaterials with enzyme-like activity, can overcome the disadvantages of natural enzymes, while retaining the unique advantages of nanomaterials such as tunable catalytic activity and type and optical, magnetic, and electrical properties, which have attracted extensive interest in recent years.[4–6] However, compared with natural enzymes, nanozymes exhibit limited catalytic activity and specificity, which restrict their practical application for the construction of analytical sensing platforms with sensitivity and selectivity. Thus, it is highly desirable to develop efficient modes to achieve highly sensitive and selective sensing for specific analytes based on nanozyme systems.

For high-quality sensing, extensive efforts have been devoted to the rational design of nanozyme structures, including altering their size,[7] controlling their morphology,[8] surface modification,[9] and changing their chemical composition.[10] Among them, modification of the surface functional groups is an efficient approach to obtain nanozymes with a superior catalytic performance.[11–14] Qu's group measured the peroxidase-like activity of graphene quantum dots after selectively deactivating their ketonic carbonyl, carboxylic, or hydroxyl groups and concluded that the –C=O groups acted as the catalytically active sites, the O=C–O– groups as the substrate-binding sites, and the –C–OH groups inhibited the activity.[11] Hwang's group

[a]*Key Laboratory of Chongqing Inorganic Special Functional Materials, College of Chemistry and Chemical Engineering, Yangtze Normal University, Chongqing 408100, PR China. E-mail: dongwenfei@yznu.edu.cn*

[b]*College of Chemistry and Chemical Engineering, Central South University, Changsha, Hunan 410083, PR China*

† Electronic supplementary information (ESI) available. See DOI: https://doi.org/10.1039/d3ra02946h

‡ These authors contribute to this work equally.

functionalized the MIL-100(Fe) nanozyme by grafting various aliphatic diamines on its coordinatively unsaturated metals sites and found that the enhanced peroxidase-like activity of amine-functionalized MIL-100(Fe) is due to the synergistic effect of the enhanced negative potential and precisely controlled molecular size of the grafted diamines.[12] Zhu's group introduced two functional groups (nitro and amino) in MIL-101(Fe) to tune its atomically dispersed metal active sites and demonstrated that functionalization with nitro ($-NO_2$) increased the peroxidase-like activity of MIL-101(Fe), whereas amino ($-NH_2$) decreased it.[13] Wei's group investigated the oxidase-like activity of a series of substituted MIL-53(Fe) with similar coordination. A Hammett-type structure–activity linear free energy relationship was observed, indicating that an increase in the Hammett sigma(m) value with electron-withdrawing ligands increases the oxidase-like activity. MIL-53(Fe)–NO_2 with the strongest electron-withdrawing NO_2 substituent showed a ten-fold higher activity than the unsubstituted MIL-53(Fe).[14] Most reports focused on the design of functional groups on nanozymes for the improvement of their catalytical performance, which is attractive for analytical sensing. Alternatively, the analytes being detected also have rich functional groups, which can significantly affect the activity of nanozymes, and thus be considered in the construction of analytical sensing platform with high sensitivity and selectivity. To date, to the best of our knowledge, research on nanozymes and the functional groups on the analytes is rare.

Inspired by these facts, herein, we investigated the response of a nanozyme to various functional groups (–COOH, –CHO, –OH, and $-NH_2$) to construct a sensing platform for specific analytes instead of anchoring these group on the nanozyme to design a high-quality nanozyme for sensing. Herein, MoS_2–MIL-101(Fe) was selected as the peroxidase nanozyme because it has intrinsic unsaturated metal sites for coordinating functional group and MoS_2 can increase the catalytic activity of MIL-101(Fe).[15] Catechol (Ph–$(OH)_2$), phthalic acid (Ph–$(COOH)_2$), 1,2-phthalic dicarboxaldehyde (Ph–$(CHO)_2$), and *o*-phenylenediamine (Ph–$(NH_2)_2$) were used as representatives with hydroxyl, carboxyl, aldehyde, and amino groups, respectively. The typical chromogenic agent 3,3′,5,5′-tetramethylbenzidine (TMB) was chosen as the peroxidase substrate. The peroxidase-like activity of MoS_2–MIL-101(Fe) was evaluated by testing its catalytic ability to convert TMB into the blue-colored oxidized TMB in the presence of H_2O_2. The effect of Ph–$(OH)_2$, Ph–$(COOH)_2$, Ph–$(CHO)_2$, Ph–$(NH_2)_2$ on the MoS_2–MIL-101(Fe)-catalyzed H_2O_2–TMB system was investigated. It was found that the "on" effect and "off" effect on the nanozyme-catalyzed system could simultaneously exist for one substance (Ph–$(OH)_2$, catechol) at different concentration levels. Dopamine, a derivative of Ph–$(OH)_2$ catechol, was selected as the analyte. Based on the results, the "on" mode and "off" mode for the dopamine based on MoS_2–MIL-101(Fe)-catalyzed H_2O_2–TMB system were proposed due to the "signal-on" effect with less DA and "signal-off" effect with excess DA (Scheme 1). In addition, the sensitivity and selectivity of the "on" mode and "off" mode were balanced and applied for the analysis of practical serum samples.

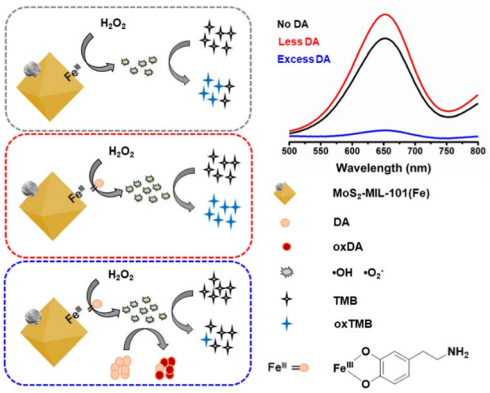

Scheme 1 Schematic diagram of the "signal-on" mode and "signal-off" mode of MoS_2–MIL-101(Fe)–H_2O_2–TMB system for less DA and excess DA.

2 Experimental

2.1 Reagents

TMB and ammonium thiomolybdate ($(NH_4)_2MoS_4$) were purchase from Sigma-Aldrich Chemical Reagent Co., Ltd. (USA). Ferric chloride hexahydrate ($FeCl_3 \cdot 6H_2O$) was obtained from Kermel Chemical Co., Ltd. (Tianjin, China). Ethanol, acetic acid (HAc) and hydrogen peroxide were provided by Chuandong Chemical Reagents Company (Chongqing, China). *N*,*N*′-Dimethylformamide (DMF) was purchased from Kelong Chemical Reagent Co., Ltd. (Chengdu, China). 1,2-Phthalic dicarboxaldehyde was provided by Sinopharm Chemical Reagent Co., Ltd. (Beijing, China). NaCl, KCl, catechol, phthalic acid, *o*-phenylenediamine, sodium acetate (NaAc), terephthalic acid, dopamine, glucose, uric acid, alanine, phenylalanine, arginine, proline, histidine, homocysteine, glutathione, and ascorbic acid were provided by Shanghai Titan Scientific Co., Ltd. (Shanghai, China). Serum samples were provided by the University Hospital (Fuling, Chongqing). Dopamine hydrochloride injections were obtained from a chemist's shop.

2.2 Instruments

Scanning electron microscopy (SEM) images of the nanozyme were recorded on a scanning electron microscope (JEOL, Japan). The transmission electron microscopy (TEM) images of the nanozyme were recorded on a TF20 field-emission transmission electron microscope at 200 kV (FEI, USA). The X-ray diffraction (XRD) patterns of the nanozyme were recorded on a Ultima IV powder X-ray diffractometer (Rigaku, Japan). The UV-vis spectra of the nanozyme catalyzed systems were recorded on a U-4100 spectrophotometer (Hitachi, Japan).

2.3 Preparation of MoS_2–MIL-101(Fe) nanocomposite

The MoS_2–MIL-101(Fe) nanocomposite was prepared based on our previous work.[15]

2.4 Determination of dopamine

The typical process for evaluating MoS_2–MIL-101(Fe) as a peroxidase mimetic was performed in acetate buffer solution

(2 mL, 0.2 M, pH 3.0) composed of 0.25 mL MoS_2–MIL-101(Fe) (50 mg L^{-1}), 0.10 mL TMB (2.5 mM in EtOH), and 0.15 mL H_2O_2 (1 mM). The MoS_2–MIL-101(Fe)-catalyzed system was incubated at 30 °C for 20 min and then its absorption spectrum was recorded using a UV-vis spectrophotometer.

A typical process for the "signal-on" mode for the determination of dopamine based on MoS_2–MIL-101(Fe) as a peroxidase mimetic was carried out by measuring the UV-vis spectra of solutions composed of acetate buffer solution (1.9 mL, 0.2 M, pH 4.0), 0.25 mL MoS_2–MIL-101(Fe) (50 mg L^{-1}), 0.10 mL TMB (2.5 mM in EtOH), 0.15 mL H_2O_2 (1 mM) in the presence of 0.10 mL different concentrations of dopamine after incubation at 30 °C for 15 min. The typical process for the "signal-off" mode was conducted by recording the UV-vis spectra of the same solutions as that in the "signal-on" mode after incubation at 40 °C for 25 min.

For practical use of the "signal-on" mode for dopamine determination, five serum samples taken from the University Hospital and two dopamine hydrochloride injections from a chemist's shop were chosen. In the case of the former, the serum samples were centrifuged at 10 000 rpm for 10 min, and then the obtained supernatant was diluted 20 times for further use. The next operation was the same as that for the typical "signal-on" dopamine determination except that the diluted serum supernatant was used in place of dopamine solution. In the case of the latter, the two dopamine hydrochloride injections were diluted 20 000 times and 10 000 times to the detectable range of "signal-on" mode, respectively. The diluted solution replaced dopamine solution for further determination.

3 Results and discussion

3.1 Characterisation of MoS_2–MIL-101(Fe)

MoS_2–MIL-101(Fe) was synthesized by growing MIL-101(Fe) crystals in the presence of as-prepared MoS_2. As shown in Fig. 1A and B, the MoS_2–MIL-101(Fe) composite appears as MoS_2 nanoparticles anchored on MIL-101(Fe) octahedra. The size of MIL-101(Fe) is not very uniform with an average size of 2.29 μm and a size in the range of 0.74 to 6.08 μm (Fig. 1A and S1†). The element mapping demonstrated the presence of Fe, O, C, Mo, and S in the composite and confirmed the structure of MoS_2 nanoparticles anchored around MIL-101(Fe) (Fig. 1C). The XRD pattern of MoS_2–MIL-101(Fe) is consistent with that of simulated MIL-101(Fe) (Fig. 1D), confirming the existence of MIL-101(Fe). Besides, the obvious characteristic peak at about 9.6° is attributed to MoS_2, indicating that MoS_2 was also maintained in the composite during the growth process of MIL-101(Fe).

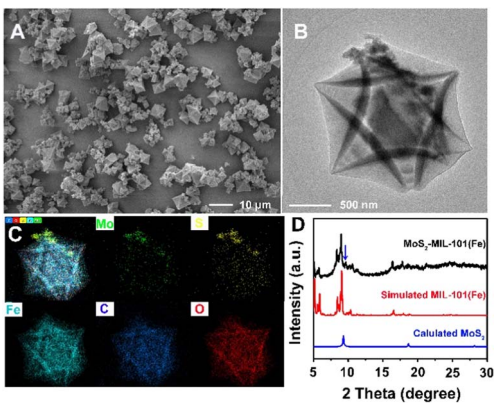

Fig. 1 (A) SEM image of MoS_2–MIL-101(Fe). (B) TEM image of MoS_2–MIL-101(Fe). (C) Element mapping of MoS_2–MIL-101(Fe). (D) XRD pattern of MoS_2–MIL-101(Fe).

3.2 The effect of groups on MoS_2–MIL-101(Fe) nanozyme-catalyzed system

In our previous report, MoS_2–MIL-101(Fe) was demonstrated to have peroxidase-like activity to catalyze the oxidation of TMB by H_2O_2 accompanied with an adsorption at 652 nm for the oxidized TMB.[15] Herein, the effect of different groups with a concentration in the range of 0.5–50 μM on the MoS_2–MIL-101(Fe) nanozyme system was investigated. Phthalic acid (Ph–$(COOH)_2$), 1,2-phthalic dicarboxaldehyde (Ph–$(CHO)_2$), catechol (Ph–$(OH)_2$), and *o*-phenylenediamine (Ph–$(NH_2)_2$) were used as representatives with carboxyl, aldehyde, hydroxyl, and amino groups, respectively. As shown in Fig. 2, an increase in Ph–$(COOH)_2$ concentration did not accelerate or decelerate the MoS_2–MIL-101(Fe) nanozyme-catalyzed H_2O_2–TMB reaction, while an increase in the concentration of Ph–$(CHO)_2$ and Ph–$(OH)_2$ at a relatively high range (higher than 8 μM) and an increase in the concentration of Ph–$(NH_2)_2$ inhibited the signal of the MoS_2–MIL-101(Fe)–H_2O_2–TMB reaction system. Moreover, the inhibition of this catalytic redox reaction increased in the order of Ph–$(COOH)_2$, Ph–$(CHO)_2$, Ph–$(OH)_2$ and Ph–$(NH_2)_2$, which can be attributed to the order of the reducing ability of these groups (–COOH < –CHO < –OH < $–NH_2$). In addition, Ph–$(OH)_2$ at a low concentration of 0.5–8 μM exhibited a promotion effect on the MoS_2–MIL-101(Fe)–H_2O_2–TMB

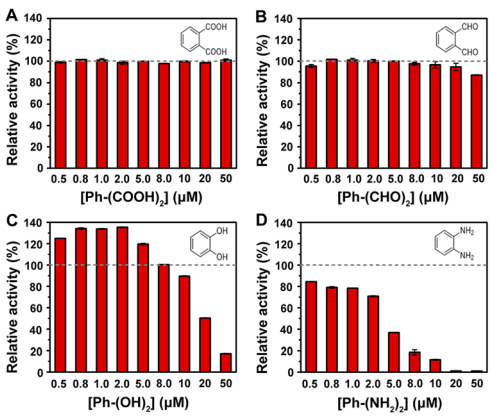

Fig. 2 Effect of Ph–$(COOH)_2$ (A), Ph–$(CHO)_2$ (B), Ph–$(OH)_2$ (C) and Ph–$(NH_2)_2$ (D) with the concentration range of 0.5–50 μM on MoS_2–MIL-101(Fe)-catalyzed H_2O_2–TMB system. The grey dash line indicates the criterion of the activity of MoS_2–MIL-101(Fe) in the H_2O_2–TMB system. The relative activity (%) means the ratio of the activity of the MoS_2–MIL-101(Fe)–H_2O_2–TMB system in the presence of various concentrations of representatives to that in the absence of these representatives.

reaction system, which differs from other representatives with groups at a low concentration of 0.5–8 μM (unchanged effect for Ph–$(COOH)_2$ and Ph–$(CHO)_2$, and inhibition effect for Ph–$(NH_2)_2$). The interaction of MoS_2–MIL-101(Fe) with Ph–$(NH_2)_2$, Ph–$(OH)_2$, Ph–$(CHO)_2$, and Ph–$(COOH)_2$ was investigated through UV-vis spectroscopy (Fig. S2†). Ph–$(NH_2)_2$ and Ph–$(OH)_2$ can efficiently coordinate with the unsaturated Fe^{III} site of MoS_2–MIL-101(Fe) due to the obvious increasing signal at about 240 nm with time, which resulted from the ligand to metal charge transfer (LMCT) after the addition of Ph–$(NH_2)_2$ and Ph–$(OH)_2$ to MoS_2–MIL-101(Fe), while inconspicuous changes were observed in the presence of Ph–$(CHO)_2$ and Ph–$(COOH)_2$, indicating the absence of or weak coordination effect. A concentration lower than 0.5 μM of Ph–$(NH_2)_2$ could also increase the absorbance signal (Fig. S3†). The above-mentioned results suggest that the formation of coordination compound groups such as –OH and $–NH_2$ at low concentration results in improved catalytic activity for the "on" effect. Simultaneously, substances with functional groups can also consume the reactive oxygen species (ROS, $^{\bullet}OH$ and $O_2^{\bullet-}$) produced by MoS_2–MIL-101(Fe) catalyzing H_2O_2,[15–18] resulting in a "off" effect. Thus, the "on" effect and "off" effect depend on the balance between the groups influencing the catalyst and groups influencing the catalytic reaction. Among the substances with groups, Ph–$(OH)_2$ exhibited a distinct "on" effect on the reaction system at a low concentration and "off" effect at a high concentration, which is promising to develop two analytical modes for substances with hydroxyl groups.

3.3 Dopamine detection for "on" and "off" modes based on MoS_2–MIL-101(Fe) nanozyme

Dopamine (DA) is an important neurotransmitter with the function of regulating the central nervous system, and its abnormal concentration in the human body is related to many diseases such as Parkinson's disease, schizophrenia, and Tourette syndrome. Thus, the detection of DA with high accuracy has considerable significance for the early diagnosis of diseases. DA contains a catechol structure with two hydroxyl groups on the benzene ring, which makes it possible to monitor the DA concentration though the MoS_2–MIL-101(Fe) nanozyme system. As seen in Fig. S4A,† similar to catechol, a low concentration of DA at 0.5 μM could trigger this chromogenic reaction to produce a deeper absorption at 652 nm, whereas a high concentration at 50 μM could lower this optical signal to obtain a weak absorption at 652 nm. In less DA, a complex of DA and MoS_2–MIL-101(Fe) was formed, which exhibited higher reactivity with H_2O_2 to produce more ROS for the oxidation of with a higher absorption at 652 nm. The kinetic behaviours of MoS_2–MIL-101(Fe) and DA-coordinated MoS_2–MIL-101(Fe) were studied by measuring the initial reaction rate by varying one substance (H_2O_2 or TMB) and fixing another substance (TMB or H_2O_2) (Fig. S5†). Their kinetic curves were well fitted by the Michaelis–Menten equation to obtain their apparent kinetic parameters (K_m and V_{max}). After complexing with DA, MoS_2–MIL-101(Fe) showed a lower K_m for TMB, indicating its stronger affinity with TMB. It was deduced that the existence of DA increased the π–π interaction to enhance its affinity with TMB, further improving the catalytic ability of the H_2O_2–TMB system. In excess DA, the fluorescence emission observed at 530 nm in the DA–MoS_2–MIL-101(Fe)–H_2O_2 system is attributed to the oxidation product of DA,[19] and the existence of TMB could impair the formation of the DA oxidation product (Fig. S4B†), indicating the competition of TMB and DA as peroxidase mimetic substrates. It was deduced that a high concentration of DA can saturate the uncoordinated Fe^{III} site of MoS_2–MIL-101(Fe) and excess DA will consume the ROS produced by the DA-coordinated MoS_2–MIL-101(Fe)-catalyzed H_2O_2 system to obtain the oxidized form of DA (Scheme 1). The competition between DA and TMB to consume ROS caused a decrease in the generation of oxidized TMB with a low absorption at 652 nm. Considering the molecular formula of dopamine with the presence of both hydroxyl and amino groups (Fig. S6A†), we investigated the effect of phenylethylamine (Ph–CH_2–CH_2–NH_2) (which has the structure of dopamine without the two hydroxyl groups, as shown in Fig. S6A†) in the concentration range of 0.5–50 μM on the MoS_2–MIL-101(Fe)-catalyzed H_2O_2–TMB system (Fig. S6B†). It was found that Ph–CH_2–CH_2–NH_2 had no impact on the system, which could eliminate the effect of the amino group in dopamine on the "signal-on" effect and "signal-off" effect, and further confirmed the effect of hydroxyl groups on the "signal-on" effect and "signal-off" effect. The differentiation of phenylethylamine in the catalytic system (inconspicuous change) with *o*-phenylenediamine (strong inhibition) originates from the different positions of the amino group. Compared with a carbon chain, benzene can provide a richer electron cloud for the amino group, and thus the amino groups bonded with benzene are more likely to be oxidized. Specifically, the amino group bonded with benzene or other benzene-like structure (aromatic amine) has much stronger reducing ability than the amino group bonded with a carbon chain (aliphatic amine), which makes this differentiation. Based on these results, the "on" mode and "off" mode for the detection of dopamine based on the MoS_2–MIL-101(Fe)-catalyzed H_2O_2–TMB system are proposed.

The "signal-on" effect of 0.5 μM DA on the nanozyme-catalyzed system with a change in pH, temperature, nanozyme concentration and reaction time was investigated to acquire the optimal conditions for DA detection in the "signal-on" mode. The responses of the "signal-on" mode for DA in the pH range of 2.5–7.0, temperature range of 10–60 °C, nanozyme concentration range of 5–30 mg L^{-1}, reaction time of 5–60 min were studied, as shown in Fig. S7A–D,† respectively. The response for DA was evaluated through the difference ($A - A_0$) between the absorbance of the nanozyme system in the presence of DA (A) and that in the absence of DA (A_0). The response reached the maximum under the conditions of pH of 4.0, temperature of 30 °C, nanozyme concentration of 5 mg L^{-1} and reaction time of 15 min. Under the optimal conditions, the absorption at 652 nm of the reaction system increased with an increase in DA concentration in the range of 0–500 nM (Fig. 3A), which indicates the typical "signal-on" mode. The enhanced absorbance difference ($A - A_0$) at 652 nm displayed a good linear relationship with the DA concentration of 0.5 to 20 nM (Fig. 3B). The

linear regression equation is $A = 0.0013[DA] + 0.4422$ ($R^2 = 0.9991$, $n = 6$) with a limit of detection (LOD) of 0.5 nM. In addition, the good linear relationship can also be monitored in the DA range of 20–500 nM (Fig. 3B) with a linear regression equation of $A = 0.0002[DA] + 0.4690$ ($R^2 = 0.9930$, $n = 7$).

In the presence of 50 μM DA, the nanozyme-catalyzed system displayed the "signal-off" effect. The responses of the "signal-off" mode for 50 μM DA in the pH range of 2.5–7.0, temperature range of 10–60 °C, the nanozyme concentration range of 5–30 mg L^{-1}, and reaction time of 5–60 min were also studied in Fig. S8A–D,† respectively. The response for DA was evaluated through the difference ($A_0 - A$) between the absorbance of the nanozyme system in the presence of DA (A) and that in the absence of DA (A_0). The maximum response was observed under the conditions of pH of 4.0, temperature of 40 °C, nanozyme concentration of 5 mg L^{-1} and reaction time of 25 min. Under the optimal conditions, the absorption at 652 nm of the reaction system decreased with an increase in the concentration of DA in the range of 0–10 μM (Fig. 3C), which indicates the typical "signal-off" mode. The inhibited absorbance difference ($A_0 - A$) at 652 nm displayed a good linear relationship with a DA concentration of 0.5 to 10 μM (Fig. 3D). The linear regression equation is $A = -0.0731[DA] + 0.8432$ ($R^2 = 0.9945$, $n = 5$) with a limit of detection (LOD) of 0.5 μM.

The detectable ranges of the "signal-on" mode and "signal-off" mode were at the nanomole and micromole levels, respectively, which suggests the higher sensitivity of the "signal-on" mode over the "signal-off" mode. The "signal-on" mode is attributed to the role of the target DA as a catalyst promotor, whereas the "signal-off" mode is ascribed to its role as the catalytic reaction inhibitor. In this system, the strong coordination ability of the hydroxyl groups in DA to the MoS_2–MIL-101(Fe) catalyst is balanced with its reduction ability in the MoS_2–MIL-101(Fe)-catalyzed H_2O_2–TMB reaction. The analytical performance of the proposed "signal-on" mode and "signal-off" mode for the detection of DA based on the MoS_2–MIL-101(Fe) system was compared with other reported methods based on nanozyme systems. It was found that the limit of detection (LOD) of the "signal-on" mode is lower than that obtained from other methods (Table 1),[20–31] indicating the superiority of the proposed "signal-on" method for sensing DA in terms of sensitivity.

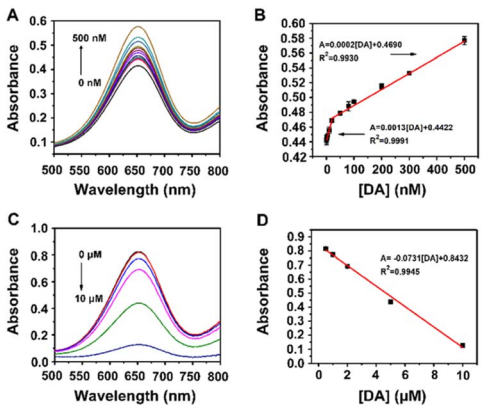

Fig. 3 (A) UV-vis spectra and (B) absorbance response of MoS_2–MIL-101(Fe)–H_2O_2–TMB system in different concentrations of DA in the "signal-on" mode. (C) UV-vis spectra and (D) absorbance response of MoS_2–MIL-101(Fe)–H_2O_2–TMB system in different concentrations of DA in the "signal-off" mode.

For practical application, selectivity experiments of the proposed "signal-on" and "signal-off" modes were also conducted by testing the response of DA and various substances (including NaCl, KCl, glucose (Glu), uric acid (UA), alanine (Ala), phenylalanine (Phe), arginine (Arg), proline (Pro), histidine (His), homocysteine (Hcy), glutathione (GSH), and ascorbic acid (AA)) at the same concentration. The DA response was not interfered by the other tested substances in the "signal-on" mode due to the strong coordination ability of the hydroxyl groups in DA with MoS_2–MIL-101(Fe) (Fig. 4A), whereas the DA response was partially affected by some tested substances with reducing ability (such as Hcy, GSH, and AA) due to the non-specific function of the redox catalytic reaction (Fig. 4B). It was noted that GSH showed a higher response than DA. GSH is type of tripeptide, which is constructed by glycine (Gly), glutamic acid (Glut) and cysteine (Cys) (Fig. S9A†). Thus, the response of Gly, Glut and Cys was also investigated (Fig. S9B†). It was found that Cys has obvious inhibition response, which is similar with GSH and higher than DA, while Gly and Glut have no obvious effect on this system. Gly and Glut have functional groups including carboxyl groups and amino groups on their carbon chains, and Cys has thiol functional groups besides carboxyl groups and amino groups. Therefore, the thiol group in GSH is the reason for the high response of the "signal-off" effect. The higher selectivity for GSH than DA is caused by the stronger reducing ability of the thiol group than hydroxyl group. Sulfur and oxygen belong to the same main group of elements, and the atomic radius of oxygen atom is greater than that of sulfur atom; thus, the sulfur atom has weaker binding ability to the outer electrons, which makes it more likely to lose electrons and be oxidized. These results confirm the higher selectivity of the "signal-on" mode over "signal-off" mode.

By balancing the "signal-on" mode and "signal-off" mode for the detection of DA, it was found that the "signal-on" mode is superior to the "signal-off" mode based on its milder reaction temperature (30 °C), shorter reaction time (15 min), and higher sensitivity and selectivity, which is applicable for practical samples.

3.4 Dopamine detection in human serum samples and dopamine hydrochloride injections using the "signal-on" mode

Human serum samples were employed to evaluate the applicability of the "signal-on" mode based on the MoS_2–MIL-101(Fe) nanozyme for detecting DA in real samples. After these samples were pre-treated according to the steps in the Experimental section, they were spiked with DA standard solution and utilized for the analysis of DA. As can be seen in Table 2, satisfactory recoveries of 91.54–112.31% were acquired for detecting DA in the human serum samples by using this "signal-

Table 1 Comparison of the proposed methods of the MoS_2–MIL-101(Fe)-catalyzed system with a "signal-on" mode and "signal-off" mode with other reported methods with nanozyme systems

Nanozyme	Method	Mode	Linear range (μM)	LOD (μM)	Ref.
Fe_3O_4@Au	Electrochemistry	Signal-on	10–1000	0.058	20
rGO–Co_3O_4	Electrochemistry	Signal-on	0–30	0.277	21
Fe–MIL-88	Fluorometry	Signal-on	0.05–30	0.046	22
β-CD@AuNCs	Fluorometry	Signal-off	0.1–80	0.02	23
Fe_3O_4 NPs	Colorimetry	Signal-on	0.010–4.0	0.0035	24
Fe/NC-800	Colorimetry	Signal-off	0.01–40	0.01	25
PtNPs@MnO_2	Colorimetry	Signal-off	0.1–1.1	0.025	26
h-CuS NCs	Colorimetry	Signal-off	2–150	1.67	27
Pt/hBNNSs-5	Colorimetry	Signal-off	2–55	0.76	28
[Cu(PDA)(DMF)]	Colorimetry	Signal-off	10–100	ND	29
Por–$CuCo_2O_4$	Colorimetry	Signal-off	10–100	0.94	30
Pt/$CoSn(OH)_6$	Colorimetry	Signal-off	5–60	0.76	31
MoS_2–MIL-101(Fe)	Colorimetry	Signal-on	0.0005–0.02, 0.02–0.5	0.0005	This work
MoS_2–MIL-101(Fe)	Colorimetry	Signal-off	0.5–10	0.5	This work

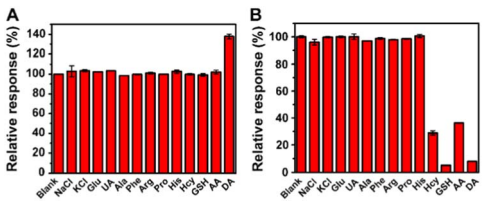

Fig. 4 (A) Selectivity experiment of the "signal-on" mode to DA and various substances at 0.5 μM. (B) Selectivity experiment of the "signal-off" mode to DA and various substances at 50 μM.

on" mode. In addition, the content of dopamine in two dopamine hydrochloride injections is also measured by "signal-on" mode (Table S1†), obtaining a consistent result with the labelled value given by the manufacturers. These results indicate the feasibility and reliability of the proposed "signal-on" mode for the detection of DA.

Table 2 Real sample analysis through the signal-on mode based on MoS_2–MIL-101(Fe) as peroxidase mimetics[a]

Sample	Detected (nM)	Spiked (nM)	Found (nM)	Recovery (%)	RSD (%) ($n = 3$)
1	N.D.	100	98.53	98.53	6.91
		300	302.20	100.73	1.63
		500	509.51	98.24	3.66
2	N.D.	100	97.31	97.31	4.88
		300	287.56	95.85	4.88
		500	476.59	95.31	3.17
3	N.D.	100	92.44	92.43	2.44
		300	319.27	106.42	3.25
		500	468.05	93.61	1.46
4	N.D.	5	5.62	112.31	7.69
		10	10.10	101.03	4.44
		20	18.31	91.54	6.66
5	N.D.	5	5.23	104.62	15.38
		10	10.23	102.31	11.54
		20	18.31	91.54	7.69

[a] N.D. means not detected.

4 Conclusion

In summary, the response of various functional groups (–COOH, –CHO, –OH, and $–NH_2$) to the MoS_2–MIL-101(Fe) nanozyme-catalyzed H_2O_2–TMB colorimetric system was investigated. The substance with –OH groups (catechol) at a low concentration could increase the signal of the catalytic system due to the strong coordination ability of the –OH groups with MoS_2–MIL-101(Fe), and catechol at a high concentration decreased the signal due to its reduction ability. The detection of DA with a catechol-like structure was proposed based on the "signal-on" mode and "signal-off" mode. By balancing these two modes, the "signal-on" mode was found to have a milder reaction temperature, shorter reaction time, and higher sensitivity and selectivity. The detectable range realized was at the nanomole level, and the LOD was as low as 0.5 nM. In addition, the proposed mode for the detection of DA could be applied to human serum samples with satisfactory recoveries and commercial injections with good accuracy. Our results will pave a pathway for designing ultrasensitive and selective methods for clinical diagnosis.

Author contributions

Hongmei Lan: investigation, methodology, writing – original draft. Gaoya Li: investigation, methodology, validation. Guo Chen: writing – original draft, visualization. Mengyao Ding: investigation, validation. Shuanglin Xiao: investigation. Jianglin Xiang: investigation. Xingwu Duan: resources. Haiyan Cao: writing – reviewing and editing. Wenbing Shi: resources, writing – reviewing and editing. Wenfei Dong: supervision, conceptualization, methodology, writing – reviewing and editing.

Conflicts of interest

There are no conflicts to declare.

Acknowledgements

The work was supported by the Natural Science Foundation of Chongqing City (cstc2020jcyj-msxmX0430), the Undergraduate

Innovation and Entrepreneurship Training Project of Chongqing City (S202110647014), the Postgraduate Scientific Research Innovation Project of Hunan Province (CX20210170) and the Fundamental Research Funds for the Central Universities of Central South University (2021zzts0069).

Notes and references

1 S. Ye, Y. Mao, Y. Guo and S. Zhang, *TrAC, Trends Anal. Chem.*, 2014, **55**, 43–54.
2 X.-m. Chen, B.-y. Su, X.-h. Song, Q.-a. Chen, X. Chen and X.-r. Wang, *TrAC, Trends Anal. Chem.*, 2011, **30**, 665–676.
3 P. Rahimi and Y. Joseph, *TrAC, Trends Anal. Chem.*, 2019, **110**, 367–374.
4 J. Wu, X. Wang, Q. Wang, Z. Lou, S. Li, Y. Zhu, L. Qin and H. Wei, *Chem. Soc. Rev.*, 2019, **48**, 1004–1076.
5 M. Liang and X. Yan, *Acc. Chem. Res.*, 2019, **52**, 2190–2200.
6 Y. Li and J. Liu, *Mater. Horiz.*, 2021, **8**, 336–350.
7 Q. Chen, S. Li, Y. Liu, X. Zhang, Y. Tang, H. Chai and Y. Huang, *Sens. Actuators, B*, 2020, **305**, 127511.
8 X. Zhang, X. Mao, S. Li, W. Dong and Y. Huang, *Sens. Actuators, B*, 2018, **258**, 80–87.
9 B. Liu and J. Liu, *Nano Res.*, 2017, **10**, 1125–1148.
10 S. Li, Y. Hou, Q. Chen, X. Zhang, H. Cao and Y. Huang, *ACS Appl. Mater. Interfaces*, 2020, **12**, 2581–2590.
11 H. Sun, A. Zhao, N. Gao, K. Li, J. Ren and X. Qu, *Angew. Chem., Int. Ed.*, 2015, **54**, 7176–7180.
12 A. H. Valekar, B. S. Batule, M. I. Kim, K.-H. Cho, D.-Y. Hong, U.-H. Lee, J.-S. Chang, H. G. Park and Y. K. Hwang, *Biosens. Bioelectron.*, 2018, **100**, 161–168.
13 W. Xu, Y. Kang, L. Jiao, Y. Wu, H. Yan, J. Li, W. Gu, W. Song and C. Zhu, *Nano-Micro Lett.*, 2020, **12**, 184.
14 J. Wu, Z. Wang, X. Jin, S. Zhang, T. Li, Y. Zhang, H. Xing, Y. Yu, H. Zhang, X. Gao and H. Wei, *Adv. Mater.*, 2021, **33**, 2005024.
15 W. Dong, G. Chen, X. Hu, X. Zhang, W. Shi and Z. Fu, *Sens. Actuators, B*, 2020, **305**, 127530.
16 S. Tamagaki, K. Suzuki and W. Tagaki, *Bull. Chem. Soc. Jpn.*, 1989, **62**, 148–152.
17 W. Li, Y. Wang and A. Irini, *Chem. Eng. J.*, 2014, **244**, 1–8.
18 C. Iuga, J. R. Alvarez-Idaboy and A. Vivier-Bunge, *J. Phys. Chem. B*, 2011, **115**, 12234–12246.
19 X. Xu, X. Zou, S. Wu, L. Wang, X. Niu, X. Li, J. Pan, H. Zhao and M. Lan, *Anal. Chim. Acta*, 2019, **1053**, 89–97.
20 H. Guan, B. Liu, D. Gong, B. Peng, B. Han and N. Zhang, *Microchem. J.*, 2021, **164**, 105943.
21 A. Numan, M. M. Shahid, F. S. Omar, K. Ramesh and S. Ramesh, *Sens. Actuators, B*, 2017, **238**, 1043–1051.
22 C. Zhao, Z. Jiang, R. Mu and Y. Li, *Talanta*, 2016, **159**, 365–370.
23 M. I. Halawa, F. Wu, T. H. Fereja, B. Lou and G. Xu, *Sens. Actuators, B*, 2018, **254**, 1017–1024.
24 M. Yin, S. Li, Y. Wan, L. Feng, X. Zhao, S. Zhang, S. Liu, P. Cao and H. Wang, *Chem. Commun.*, 2019, **55**, 12008–12011.
25 Q. Chen, C. Liang, X. Zhang and Y. Huang, *Talanta*, 2018, **182**, 476–483.
26 J. Liu, L. Meng, Z. Fei, P. J. Dyson and L. Zhang, *Biosens. Bioelectron.*, 2018, **121**, 159–165.
27 J. Zhu, X. Peng, W. Nie, Y. Wang, J. Gao, W. Wen, J. N. Selvaraj, X. Zhang and S. Wang, *Biosens. Bioelectron.*, 2019, **141**, 111450.
28 M. N. Ivanova, E. D. Grayfer, E. E. Plotnikova, L. S. Kibis, G. Darabdhara, P. K. Boruah, M. R. Das and V. E. Fedorov, *ACS Appl. Mater. Interfaces*, 2019, **11**, 22102–22112.
29 J. Wang, Y. Hu, Q. Zhou, L. Hu, W. Fu and Y. Wang, *ACS Appl. Mater. Interfaces*, 2019, **11**, 44466–44473.
30 Y. He, N. Li, X. Liu, W. Chen, X. Zhu and Q. Liu, *Microchim. Acta*, 2021, **188**, 171.
31 H. Liu, Y.-N. Ding, B. Bian, L. Li, R. Li, X. Zhang, Z. Liu, X. Zhang, G. Fan and Q. Liu, *Microchim. Acta*, 2019, **186**, 755.